Supplemental Information

Material and Methods

Cell culture. The human osteosarcoma cell line, HOS, was obtained from Dr. Richard Schwartz (Michigan State University, East Lansing, MI) and grown in Dulbecco's modified Eagle's medium (Invitrogen, Carlsbad, CA) supplemented with 5% (v/v) fetal bovine serum, 5% newborn calf serum, and penicillin (50 units/mL) plus streptomycin (50 µg/mL; Quality Biological, Gaithersburg, MD).

Vector Constructs and mutagenesis. pNLNgoMIVR-ΔEnv.LUC has been described previously [1]. The region comprising the RT open reading frame was removed from pNLNgoMIVR-ΔEnv.LUC (by digestion with SpeI and SalI) and inserted between the SpeI and SalI sites of pBluescript II KS+. Using that construct as the template, We prepared the following NNRTI resistant mutations in HIV-1 RT using the QuikChange II XL (Stratagene, La Jolla, CA) site-directed mutagenesis protocol: L100I, K103N, Y181C, Y188L, H221Y, K103N/Y181C, G190A, G190S, M230L, P236L, L100I/K103N, K103N/P225H, V106A/G190A/F227L, V106A, L234I, V106A/F227L, V106A/L234I, V106A/F227L/L234I, E40K, D67E, K101E, V111A, E138K, M184I, M184V, K101E/M184I, K101E/M184V, E138K/M184I, E138K/M184V, K101P, Y181I, and K101P/V179I. The following sense mutagenic oligonucleotides were used with cognate antisense oligonucleotides (not shown) (Integrated DNA Technologies, Coralville, IA) in the mutagenesis: L100I, 5'-CATCCCGCAGGGATAAAAAAGAAAAAATCA-3'; L100I 2-103, 5'-ATACCACATCCCGCAGGGATTAAAAAGAATAAATCAGTA-3'; K103N, 5'-GCAGGGTTAAAAAAGAATAAATCAGTAACAGTA-3'; Y181C, 5'-CCAGACATAGTTATCTGTCAATACATGGATGAT-3'; Y188L, 5'-TACATGGATGATTTGCTAGTAGGATCTGACTTA-3'; H221Y, 5'-ACACCAGACAAAAAATATCAGAAAGAACCTCCA-3'; G190A, 5'-ATGGATGATTTGTATGTAGCATCTGACTTAGAAATAGGG-3'; G190S, 5'-ATGGATGATTTGTATGTAAGTTCTGACTTAGAAATAGGG-3'; P225H, 5'-AAAAAACATCAGAAAGAACATCCATTCCTTTGGATGGGT-3'; F227, 5'-

CATCAGAAAGAACCTCCATTACTTTGGATGGGTTATGAA-3’; M230L, 5’-GAACCTCCATTCCTTTGGCTGGGTTATGAACTCCATCCT-3’; P236L, 5’-ATGGGTTATGAACTGCATCTCGATAAATGGACAGTACAG-3’; V106A, 5’-AAAAAGAAAAAATCAGCAACAGTACTGGATGTG-3’; L234I, 5’-TTCCTTTGGATGGGTTATGAAATCCATCCTGATAAATGGACAGTA-3’; E40K, 5’-GAAATTTGTACAAAAATGGAAAAGGAAGGG-3’; D67E, 5’- GCCATAAAGAAAAAAGAAAGTACTAAATGGAGA-3’; K101E, 5’-CATCCCGCAGGGTTAGAAAAGAAAAAATCAGTAACA-3’; V111A, 5’-GTAACAGTACTGGATGTAGGTGATGCATATTTTTCA-3’; E138K, 5’-CCTAGTATAAACAATAAGACACCAGGGATTAGA-3’; M184I, 5’-GTTATCTATCAATACATAGATGATTTGTATGTA-3’; M184V, 5’-GTTATCTATCAATACGTTGATGATTTGTATGTA-3’; K101P, 5’-CCACATCCCGCAGGGTTACCAAAGAAAAAATCAGTAACA-3’; Y181I, 5’-AATCCAGACATAGTTATCATTCAATACATGGATGATTTG-3’; K101P/V179I, 5’-AAACAAAATCCAGACATAATCATCTATCAATACATGGAT-3’. The double mutants K103N/Y181C, K103N/P225H, and L100I/K103N were created by using the previously generated K103N mutant and the appropriate oligonucleotides for the second mutation, Y181C, P225, and L100I respectively. The double mutants V106A/F227L and V106A/L234I were constructed by using the previously generated V106A mutant and the appropriate oligonucleotides for the second mutation, F227L and L234I, respectively. The double mutants K101E/M184I and K101E/M184V were constructed by using the previously generated K101E mutant and the appropriate oligonucleotides for the second mutation, M184I and M184V, respectively. The double mutants E138K/M184I and E138K/M184V were constructed by using the previously generated E138K mutant and the appropriate oligonucleotides for the second mutation, M184I and M184V, respectively. The triple mutant V106A/F227L/L234I was made by using the previously generated V106A/F227L double mutant and the appropriate oligonucleotides for the third mutation, L234I. The triple mutant V106A/G190A/F227L was constructed in a series of steps by using

the previously generated V106A mutant and the appropriate oligonucleotides for the second mutation, G190A, to generate the double mutant V106A/G190A, and then the triple mutant was made by using double mutant V106A/G190A and oligonucleotides for the third mutation, F227L. The DNA sequence of each construct was verified independently by DNA sequence determination. The mutated RT coding sequences from pBluescript II KS+ were then subcloned into pNLNgoMIVR-ΔEnv.LUC (between the KpnI and SalI sites) to produce mutant HIV-1 constructs and checked by DNA sequencing.

Selection of NNRTI mutations in HIV-1. HuT-CCR5 cells were infected with HIV-1_{LAI} for 2 hours at a multiplicity of infection of 0.1-0.01. Cells were cultured in the presence or absence of RPV or a closely related compound to RPV. Viral RNA from the supernatant was isolated and used as template in RT-PCR assays with primers spanning the RT coding region. PCR product was sequenced to identify any mutations.

Computer Modeling. All computer modeling was performed using MOE2014.09 (Chemical Computing Group, Montreal, Quebec, Canada). All modeling of RPV and DOR in the NNRTI binding pocket were made from previously published crystal structures of a WT HIV-1 RT/RPV complex (PDB ID: 2ZD1; [2]) and a WT HIV-1 RT/DOR complex (PDB ID: 4NCG; [3, 4]).

References

1. Zhao, X.Z., et al., *2,3-dihydro-6,7-dihydroxy-1H-isoindol-1-one-based HIV-1 integrase inhibitors.* J Med Chem, 2008. **51**(2): p. 251-9.
2. Das, K., et al., *High-resolution structures of HIV-1 reverse transcriptase/TMC278 complexes: strategic flexibility explains potency against resistance mutations.* Proc Natl Acad Sci U S A, 2008. **105**(5): p. 1466-71.
3. Lai, M.T., et al., *In vitro characterization of MK-1439, a novel HIV-1 nonnucleoside reverse transcriptase inhibitor.* Antimicrob Agents Chemother, 2014. **58**(3): p. 1652-63.
4. Feng, M., et al., *In vitro resistance selection with doravirine (MK-1439), a novel nonnucleoside reverse transcriptase inhibitor with distinct mutation development pathways.* Antimicrob Agents Chemother, 2015. **59**(1): p. 590-8.

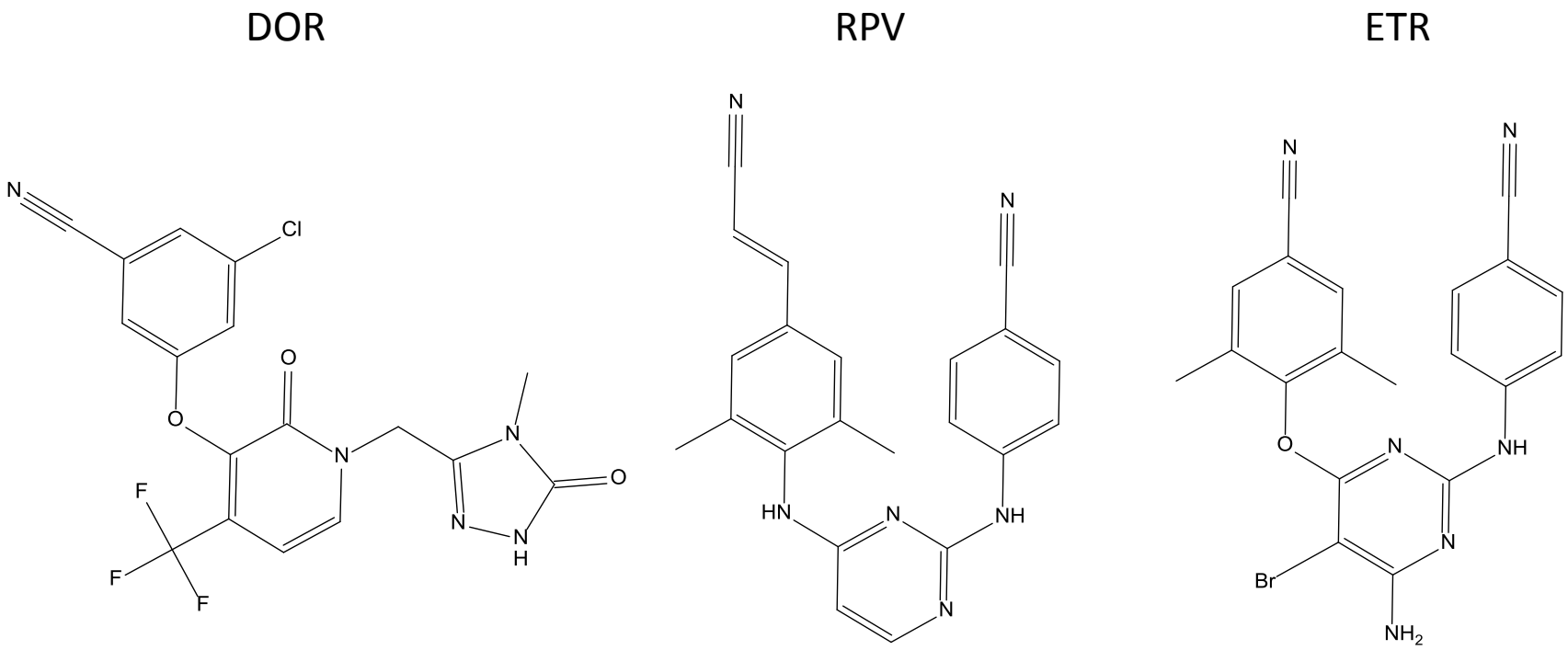

Supplementary Figure 1. Chemical Structures of DOR, RPV, and ETR
The chemical structures of DOR, RPV, and ETR.

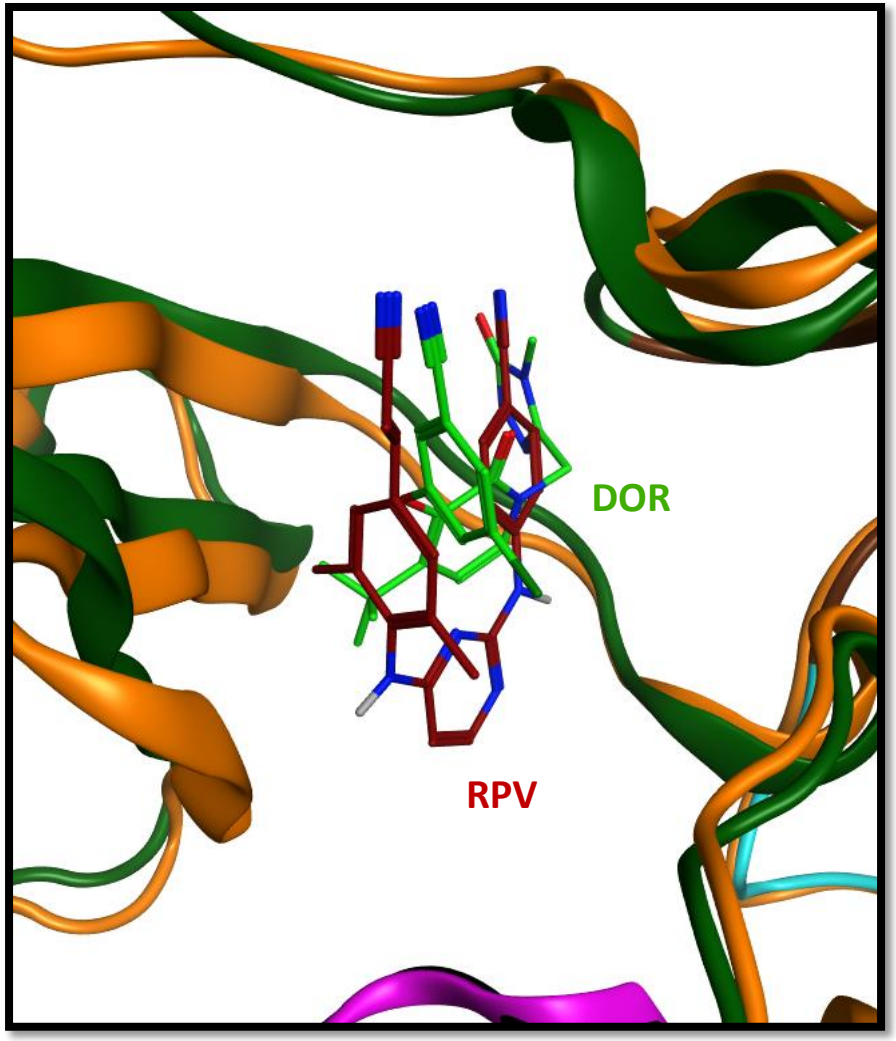

Supplementary Figure 2. Comparing the relative positions of RPV and DOR in the NNRTI binding pocket The positions of DOR (light green) and RPV (maroon) in the NNRTI binding pocket are shown with the backbone of the p66 subunit (shown in orange for DOR, dark green for RPV) and the backbone of the p51 subunit of RT (shown in magenta for DOR, black for RPV) at the bottom of the image. The pyrimidine scaffold of DOR sits between 1.25-1.5 Å deeper than that of RPV.